# SDA Full-Wave Analysis of Boxed Multistrip Superconducting Lines of Finite Thickness Embedded in a Layered Lossy Medium

Anatoli N. Deleniv, Marina S. Gashinova, and Irina B. Vendik, *Member, IEEE*

***Abstract*—The spectral-domain approach is applied to modeling propagation characteristics of a multiconductor structure of superconducting strip lines with signal strips and ground planes of finite thickness in lossy layered media. Two sets of basis functions (Chebyshev and Legendre polynomials) are compared by their ability for accurate modeling of microwave losses. Simple expressions within the immitance approach are presented for a power flux computation. As a result, complex propagation constants and related modal impedances of a multiconductor structure containing superconducting strips can be calculated with a high accuracy. The model applicability is illustrated by numerical results compared with available simulated data.**

***Index Terms*—Modal impedance, multilayered media, multistrip lines, spectral-domain approach, superconductor.**

## I. Introduction

HIGH-TEMPERATURE superconductors (HTS) are promising for microwave applications due to low surface resistance and frequency-independent penetration depth. These properties make them attractive in a development of some devices like multipole narrow-band filters with a low in-band insertion loss and sharp skirts, multiplexers, and others [1]. An important point in synthesis of such devices is an accurate estimation of guided-wave propagation characteristics, namely, complex propagation constants and related modal impedances. In order to provide the desired accuracy, the HTS macroscopic electrical parameters, such as complex conductivity and field penetration depth, have to be taken into account.

HTS planar transmission lines were the subject of interest for many investigators. This type lines have been analyzed on isotropic [2]–[6], as well as anisotropic [7] substrates. A spectral-domain volume-integral equation (SDVIE) method has been proposed to analyze superconducting lines [5], [6]. The method rigorously accounts for the finite volume of the superconductors, providing accurate characterization of the kinetic inductance and conductor loss contribution. In [2], Mao *et al.*use a modified spectral-domain approach (SDA) to model all three components of strip current. As was shown, this approach provides an accurate modeling, but similarly to SDVIE, becomes computationally expensive for analysis of multiconductor system. Nghiem *et al.* also used SDA [4] to study microstrip lines and striplines. Piecewise-constant pulses are chosen to model the axial current density. It is important to note that this method could properly account for propagation parameters of a single line, but becomes computationally inefficient, whatever large number of strips or fine current resolution are subjects of interest. From this point-of-view, the use of continuous basis functions is more desirable. Lee *et al.* [7] use a concept of equivalent surface impedance based on the knowledge of current density distribution in the single strip. It is important to note that accuracy of this approach is questionable if ground-to-strip distance is small for either set of strongly coupled strips to be analyzed (for these situations, the current of the isolated strip cannot be considered as a good approximation). Pond *et al.* [3] applied the SDA to analyze superconductor microstrip lines using basis functions that incorporates singular behavior of the current at the strip edges. This choice seems to be the best approximation for a real superconductor strip; however, the formulation used in [3] is connected with the appearance of divergent series [8].

A quasi-static description of the multicoupled superconducting lines was used in the computer-aided design (CAD) tool derived for a design of filters based on sections of multicoupled lines [9]. In this paper, a further development of modeling characteristics of HTS multistrip lines is presented. An efficient SDA-based full-wave method is derived to calculate complex propagation parameters of the boxed multiconductor superconducting planar lines embedded in a loss layered isotropic media. Two sets of basis functions are tested to check their ability for an accurate description of conductor losses in a superconducting strip of finite thickness. Few simple expressions are presented to provide a connection between tangential fields at the electrode interface and at any other one. They are used for a computation of the Poynting's vector for each propagating mode and, thus, the multiport impedance (admittance) matrix. The accuracy and usefulness of the developed model is demonstrated via comparison with available numerical and experimental data.

Manuscript received May 15, 2001.

A. N. Deleniv is with the Department of Microelectronics, Chalmers University of Technology, S-41296 Göteborg, Sweden.

M. S. Gashinova and I. B. Vendik are with the Department of Microelectronics and Radio Engineering, St.-Petersburg Electrotechnical University, St.-Petersburg 197376, Russia.

Digital Object Identifier 10.1109/TMTT.2002.806907

## II. Analysis

The cross section of the multiconductor transmission structure is shown in Fig. 1.

The structure consists of $i = 1, \ldots, I$ upper and $j = 1, \ldots, J$ lower dielectric layers in reference to the electrode interface

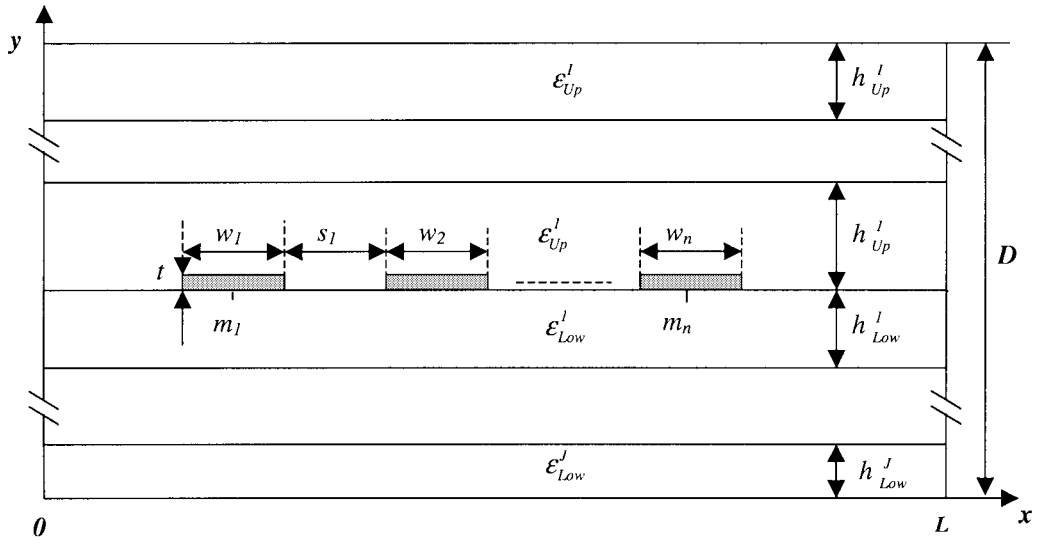


Fig. 1. Transverse section of multistrip structure in layered media.

containing $k = 1, \ldots, n$ superconducting strips. The dielectric layers are characterized by the thickness $h^i_{\mathrm{Up}}$, $h^j_{\mathrm{Low}}$ and the complex dielectric permittivity

$$\varepsilon^{i(j)}_{\mathrm{Up(Low)}} = \varepsilon_0 \varepsilon_r^{i(j)} \left(1 - j \tan \delta^{i(j)}\right) \tag{1a}$$

while for the superconductor, we use

$$\varepsilon^{i(j)}_{\mathrm{Up(Low)}} = -\frac{j\sigma_{\mathrm{sc}}}{\omega} \tag{1b}$$

with

$$\sigma_{\mathrm{sc}} = \sigma_n - j\,\frac{1}{\omega \mu_0 \lambda_L^2}. \tag{2}$$

$\sigma_{\mathrm{sc}}$ is the complex conductivity of a superconductor determined in accordance with the two-fluid model of superconductivity [10], $\sigma_n$ is the normal conductivity, $\lambda_L$ is the London penetration depth, and $\mu_0$ is the magnetic permeability of vacuum.

The goal of the analysis is to define a vector of complex propagation constant $k_z(\omega) = \beta(\omega) - j\alpha(\omega)$ in the wave-propagation direction $z$ ($\beta$ is the phase constant and $\alpha$ is the attenuation constant) and modal impedances for each mode of the structure.

### *A. Consideration of Losses in Dielectric Layers and Grounds*

We use the analytical procedure for evaluation of spectral dyad based on the so-called immitance approach [11]. The recursive use of the formula for the input admittance of the loaded line section for both TE-to-$y$ and TM-to-$y$ waves enables to build flexible codes for an arbitrary number of upper and lower layers related to the electrode interface. An extension to the lossy case is made by use of complex permittivity $\varepsilon^{i(j)}$ (1a), (1b) for the $i$th ($j$th) layer and the complex propagation constant $k_z$. For the normal metal ground, the conductivity $\sigma_{\mathrm{sc}}$ in (2) must be replaced by $\sigma_n$ of normal metal.

As losses in the dielectric and superconductor (conductor) layers are rigorously taken into account in Green's dyad, the loss contribution due to the superconducting strip conductivity needs special care for a description.

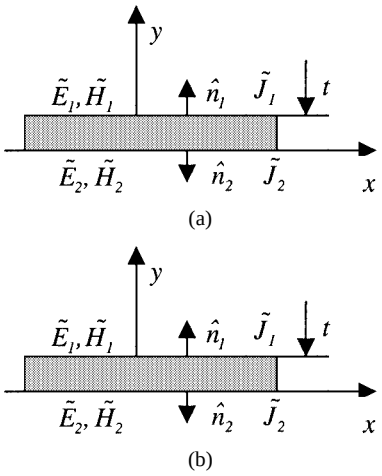


Fig. 2. Equivalence between tangential boundary conditions for: (a) the strip of thickness $t$ and (b) the infinitely thin equivalent [12].

### *B. Equivalent Surface Impedance of a Superconducting Strip*

Let us consider two superconducting strip structures, as shown in Fig. 2.

The strips differ by their thickness: the real superconducting strip is of thickness $t$ [see Fig. 2(a)] and the equivalent strip is infinitely thin [see Fig. 2(b)]. The original strip is characterized by the tangential electric- and magnetic-field components[1] on the upper and lower interfaces related by the impedance matrix of a thin conducting layer

$$\begin{bmatrix} \tilde{E}_1 \\ \tilde{E}_2 \end{bmatrix} = \hat{n}_1 \times \begin{bmatrix} Z_{11} & -Z_{12} \\ Z_{21} & -Z_{22} \end{bmatrix} \begin{bmatrix} \tilde{H}_1 \\ \tilde{H}_2 \end{bmatrix} \tag{3}$$

$$Z_{11} = Z_{22} = \frac{-j\omega\mu_0}{\beta_{\mathrm{sc}}} \cot(\beta_{\mathrm{sc}} t) \tag{4}$$

$$Z_{12} = Z_{21} = \frac{-j\omega\mu_0}{\beta_{\mathrm{sc}}} \csc(\beta_{\mathrm{sc}} t) \tag{5}$$

[1]The symbols with a tilde correspond to Fourier transforms of functions.

where $\beta_{\rm sc}$ is the complex propagation constant of the superconductor

$$\beta_{\rm sc} = \left(-j\omega\mu_0\sigma_n - \frac{1}{\lambda_L^2}\right)^{1/2}. \tag{6}$$

In the present approach, we assume that conductor losses are mostly due to the longitudinal electric current (it is true for quasi-TEM modes). Under this condition, the expressions for the $x$-component of the magnetic fields upper and lower to the strip interface can be derived using the immitance approach [11] as

$$\tilde{H}_1^x = -\left(\frac{k_z^2}{\alpha_n^2+k_z^2}\,\frac{\tilde{Y}^e_{\rm Up}}{\tilde{Y}^e_{\rm Up}+\tilde{Y}^e_{\rm Low}} + \frac{\alpha_n^2}{\alpha_n^2+k_z^2}\,\frac{\tilde{Y}^h_{\rm Up}}{\tilde{Y}^h_{\rm Up}+\tilde{Y}^h_{\rm Low}}\right)\tilde{J}_z = \tilde{K}_H^{\rm Up}\tilde{J}_z \tag{7}$$

$$\tilde{H}_2^x = \left(\frac{k_z^2}{\alpha_n^2+k_z^2}\,\frac{\tilde{Y}^e_{\rm Low}}{\tilde{Y}^e_{\rm Up}+\tilde{Y}^e_{\rm Low}} + \frac{\alpha_n^2}{\alpha_n^2+k_z^2}\,\frac{\tilde{Y}^h_{\rm Low}}{\tilde{Y}^h_{\rm Up}+\tilde{Y}^h_{\rm Low}}\right)\tilde{J}_z = \tilde{K}_H^{\rm Low}\tilde{J}_z \tag{8}$$

with $\tilde{Y}^{e(h)}_{\rm Up(Low)}$ being the input admittances for the TM-to-$y$ (TE-to-$y$) wave looking up (down) from the strip interface. In the next step, we insert (7) and (8) into (3) and obtain the following expression for the perturbed electric field on the upper and lower surfaces of the strip

$$\begin{bmatrix}\tilde{E}_1^z\\ \tilde{E}_2^z\end{bmatrix} = \hat{n}_1 \times \begin{bmatrix}Z_{11} & -Z_{12}\\ Z_{21} & -Z_{22}\end{bmatrix}\begin{bmatrix}\tilde{K}_H^{\rm Up}\\ \tilde{K}_H^{\rm Low}\end{bmatrix}\tilde{J}_z. \tag{9}$$

Expression (9) can now be used to define the impedance boundary condition for the equivalent infinitely thin strip [see Fig. 2(b)] as the weighted average [12]

$$\tilde{E}_z^{\rm strip} \approx \left(\tilde{E}_1^z,\, \tilde{E}_2^z\right) = \left(\frac{\left|\tilde{E}_1^z\right|\tilde{E}_1^z + \left|\tilde{E}_2^z\right|\tilde{E}_2^z}{\left|\tilde{E}_1^z\right| + \left|\tilde{E}_2^z\right|}\right) = \tilde{Z}_s^{\rm eq.}\tilde{J}_z. \tag{10}$$

It is important to remember that $\tilde{Z}_s^{\rm eq.}(\alpha_n)|_{n\to\infty} \to const$.

### C. Propagation Constants of the Structure Figures

The linear relationships between fields and currents at the conductor interface can be written as

$$\begin{bmatrix}\tilde{E}_z^{\rm strip}+\tilde{E}_z^{\rm ext.}\\ \tilde{E}_x^{\rm strip}+\tilde{E}_x^{\rm ext.}\end{bmatrix} = \begin{bmatrix}\tilde{Z}_{zz} & \tilde{Z}_{zx}\\ \tilde{Z}_{xz} & \tilde{Z}_{xx}\end{bmatrix}\begin{bmatrix}\tilde{J}_z\\ \tilde{J}_x\end{bmatrix} \tag{11}$$

with $\tilde{E}^{\rm strip}_{z(x)}, \tilde{E}^{\rm ext.}_{z(x)}$ being the $z(x)$ component of the electric field on the strip surface and its exterior, respectively. In the performing solution for planar transmission lines by a spectral-domain moment method, one needs to expand the unknown electric currents of the system in an $N$-dimensional basis set. We consider two different sets $\varphi 1$ and $\varphi 2$, studying a possibility to model losses in conducting strips with high accuracy. In our codes, we use the same set to model both the axial current density and derivative of the transverse one

$$J_z(x) = \sum_k \sum_p a_p^k \varphi_p^k(x) \tag{12}$$

$$J_x'(x) = \sum_k \sum_p b_p^k \varphi_p^k(x) \tag{13}$$

with $\varphi_p^k(x) \equiv \varphi 1_p^k(x)$ or $\varphi_p^k(x) \equiv \varphi 2_p^k(x)$.

The set $\varphi 1$ is the first-type Chebyshev polynomials $T_p$ with Maxwell weighting function

$$\varphi 1_p^k(x) = \begin{cases} \dfrac{2}{\pi w_k}\,\dfrac{T_p\left(\dfrac{x-m_k}{0.5w_k}\right)}{\sqrt{1-\left(\dfrac{x-m_k}{0.5w_k}\right)^2}}, & \text{for } x \in w_k\\ 0, & \text{for } x \notin w_k\end{cases} \tag{14}$$

where $k = 1, \ldots, n$ stands for the $k$th strip, and $p$ stands for the order of the basis function; $m_k$ is the position of the $k$th strip center (Fig. 1). The defined basis set is regarded as very suitable for the analysis based on SDA formulation and provides a very quick convergence pattern in terms of the basis function number, but on the other hand, it does not support a description of the finite edge current.

The set $\varphi 2$ is based on orthogonal Legendre polynomials $P_p$ and is suitable for modeling the finite edge current. With notations similar to (14), we have

$$\varphi 2_p^k(x) = \frac{1}{w_k}\,P_p\left(\frac{x-m_k}{0.5w_k}\right). \tag{15}$$

In order to apply Galerkin's method, the system of linear equations (11) has to be rearranged to a homogeneous one. Inserting (10) into (11), we formulate two different systems to be solved using the sets (15) or (14) (we consider that $\tilde{E}^x_{\rm strip} \approx 0$). The first system of equations is written as

$$\begin{bmatrix}\tilde{E}_z^{\rm ext.}(\alpha_n)\\ \tilde{V}_x^{\rm ext.}(\alpha_n)\end{bmatrix} = \begin{bmatrix}\tilde{Z}_{zz}-\tilde{Z}_s^{\rm eq.} & \dfrac{\tilde{Z}_{zx}}{-j\alpha_n}\\ \dfrac{\tilde{Z}_{xz}}{-j\alpha_n} & \dfrac{\tilde{Z}_{xx}}{-\alpha_n^2}\end{bmatrix}\begin{bmatrix}\tilde{J}_z(\alpha_n)\\ \tilde{J}_x'(\alpha_n)\end{bmatrix} \tag{16}$$

where

$$V_x(x) = \int_{-L}^{x} E_x(x')\,dx'. \tag{17}$$

The second system is written as

$$\begin{bmatrix}II\tilde{E}_z^{\rm ext.}(\alpha_n)\\ \tilde{V}_x^{\rm ext.}(\alpha_n)\end{bmatrix} = \begin{bmatrix}\dfrac{\tilde{Z}_{zz}-\tilde{Z}_s^{\rm eq.}}{-\alpha_n^2} & \dfrac{\tilde{Z}_{zx}}{j\alpha_n^3}\\ \dfrac{\tilde{Z}_{xz}}{-j\alpha_n} & \dfrac{\tilde{Z}_{xx}}{-\alpha_n^2}\end{bmatrix}\begin{bmatrix}\tilde{J}_z(\alpha_n)\\ \tilde{J}_x'(\alpha_n)\end{bmatrix} \tag{18}$$

where

$$IIE_z(x) = \int_{-L}^{x}\int_{-L}^{x'} E_z(x'')\,dx''\,dx'. \tag{19}$$

The both systems can be presented in general form as follows:

$$\left[\tilde{Y}(\alpha_n)\right] = \left[\tilde{F}(\alpha_n, \omega, k_z)\right]\left[\tilde{X}(\alpha_n)\right]. \tag{20}$$

Galerkin's method becomes inefficient being applied to solve (16) with the set $\varphi 1$ (Chebyshev polynomials) due to the appearance of divergent series [7], [8]. This problem can be avoided by use of another orthogonal set exhibiting better convergency, i.e., a higher decay rate in the Fourier region (e.g., the set $\varphi 2$ based on Legendre polynomials) to find projection of the left-hand side of (16), with the set $\varphi 1$ remaining on the right-hand side. The alternative formulation (18) gives a convergent solution with Chebyshev polynomials. The double integration of $E_z(x)$ over $x$ (19) is used to build more efficient computer codes,

though the single integration can also provide convergent solution.

Solving (20) by Galerkin's method leads to a homogeneous system of linear equations

$$[A(\omega, k_z)][X] = 0 \tag{21}$$

with coefficient matrix $[A(\omega, k_z)]$ and $[X] \equiv a_p^k \cup b_p^k$ being the unknown expansion coefficients of (12) and (13). The entries of $[A(\omega, k_z)]$ are numerical series, whose general term in (21) is

$$A_{p,q,\nu}^{k,j,\mu} = \frac{1}{Nr(p,k)} \sum_n \tilde{\varphi}_p^k(\alpha_n)^* \tilde{F}_{\mu\nu}(\alpha_n, \omega, k_z)[\tilde{\varphi}_q^j(\alpha_n)] \tag{22}$$

where $\mu(\nu)$ stands for $x$- or $z$-components of the spectral dyad, $k = 1, \ldots, n$ and $j = 1, \ldots, n$ are the strip numbers, and

$$Nr(p,k) = \sum_n \tilde{\varphi}_p^k(\alpha_n)[\tilde{\varphi}_p^k(\alpha_n)]^*. \tag{23}$$

The complex propagation constants can be found if the nontrivial solution to (21) is obtained. This corresponds to the condition

$$\det[A(\omega, k_z)] = 0 \tag{24}$$

which is actually a dispersion equation. For each particular value of $\omega$, a nontrivial solution exists for a discrete set $\{k_z^n\}$.

Solving (21) requires multiple evaluations of $[A(\omega, k_z)]$. In order to reduce numerical efforts, we implemented an effective speed-up algorithm [13] in the case of using the basis function set $\varphi 1$, while for the set $\varphi 2$, we used a large argument approximation for Legendre polynomial basis functions. In both cases, the calculation of (22) is based on the extraction of the asymptotic form of $\tilde{F}_{\mu\nu}(\alpha_n, \omega, k_z)$.

We have found that the matrix element $A_{p,q,z}^{k,k,z}$ (22) related to the asymptotic form of $\tilde{Z}_s^{\text{eq}}(\alpha_n)$ in (18) can be defined in a closed form using (25). The use of (25) in computation of the matrix $[A(\omega, k_z)]$ reduces numerical efforts of the analysis

$$\sum_{n=1}^{\infty} \frac{\tilde{\varphi}1_p^k(\alpha_n)^* \tilde{\varphi}1_q^k(\alpha_n)}{\alpha_n^2} = \frac{L}{2}\frac{w_k}{\pi^2}\left[1 + \frac{(-1)^{p+q}}{[(p+q)^2+1][(p-q)^2+1]}\right], \quad p \neq 0; \quad q = 0, 1, \ldots, N-1. \tag{25}$$

### *D. Calculation of Associated Power Flux and Modal Impedances*

It is well known that the reliability of a simulated network response is highly sensitive to accuracy of related sub-circuits characteristics: impedance, admittance, or scattering parameters. In this connection, an accurate computation of complex modal power associated with each propagating mode is important for a correct definition of impedance parameters for a multicoupled line.

Cano *et al.* [14] presented a unified way for computation of the power flux associated with the quasi-TEM modal spectrum. Using an SDA transverse propagation matrix (TPM) technique, they derived an expression for the flux of Poynting's vector as

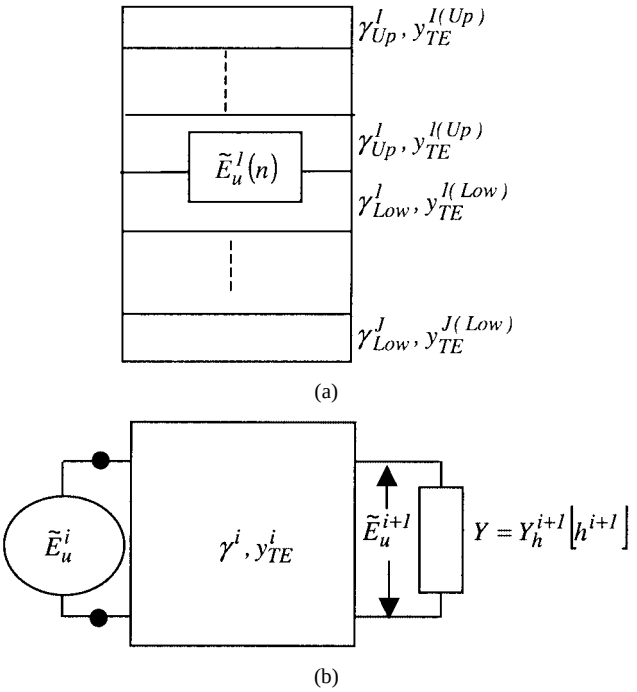


Fig. 3. Equivalent circuit for TE-to-$y$ fields for the: (a) general structure and (b) $i$th layer. $Y_{h(e)}^{i+1}(h^{i+1})$ is the input load admittance for TE(TM) waves seen from the $i$th layer toward the $(i+1)$th one.

a function of the transformed tangential electrical fields at the surfaces limiting the $i$th layer $\tilde{E}_i(\alpha_n)$ and $\tilde{E}_{i-1}(\alpha_n)$

$$P_i^k = \frac{L}{2\omega\mu_0} \sum_{n=-\infty}^{\infty} \begin{bmatrix} \tilde{E}_i^T & \tilde{E}_{i-1}^T \end{bmatrix} \left[M(\omega, \alpha_n, k_z^k)\right] \begin{bmatrix} \tilde{E}_i^* \\ \tilde{E}_{i-1}^* \end{bmatrix} \tag{26}$$

where index $k$, superscript $T$, and $*$ denote the $k$th mode, transpose, and complex conjugate, respectively. For the details related to the form of matrix $[M]$, we refer the reader to [14]. Herein, we propose an alternative to the TPM technique set of simple expressions providing a connection between tangential electric fields at the strips interface and any other one. This set can be used for an efficient computation of (26) and for the analysis of structures with electrodes in different interfaces.

Let us direct our attention to Fig. 3(a). Each layer is characterized by a transverse propagation constant in the $y$-direction $\gamma_{\text{Up(Low)}}^{i(j)}$ and TE(TM) characteristic admittances $y_{\text{TE}}^{i(j)}$, $y_{\text{TM}}^{i(j)}$ [11, eq. (10) and (11)]. With given propagation constants, tangential electric-field sources at the strip interface for TE-to-$y$ and TM-to-$y$ modes are

$$\begin{bmatrix} \tilde{E}_u^1(\alpha_n) \\ \tilde{E}_v^1(\alpha_n) \end{bmatrix} = [T] \begin{bmatrix} \tilde{E}_z^1(\alpha_n) \\ \tilde{E}_x^1(\alpha_n) \end{bmatrix} \tag{27}$$

where $[T]$ is the transformation matrix from $\boldsymbol{z}, \boldsymbol{x}$ to the $\boldsymbol{u}, \boldsymbol{v}$ coordinate system [11, eq. (10)]. It can be easily shown that with a given field source $\tilde{E}_u^i(\tilde{E}_v^i)$ [see Fig. 3(b)], the second port field $\tilde{E}_u^{i+1}$ may be expressed as

$$\tilde{E}_{u(\nu)}^{i+1} = \frac{y_{\text{TE(TM)}}^i}{y_{\text{TE(TM)}}^i \cosh(\gamma^i h^i) + Y_{h(e)}^{i+1}(h^{i+1}) \sinh(\gamma^i h^i)} \tilde{E}_{u(\nu)}^i = K_{u(v)}^i \tilde{E}_{u(\nu)}^i \tag{28}$$

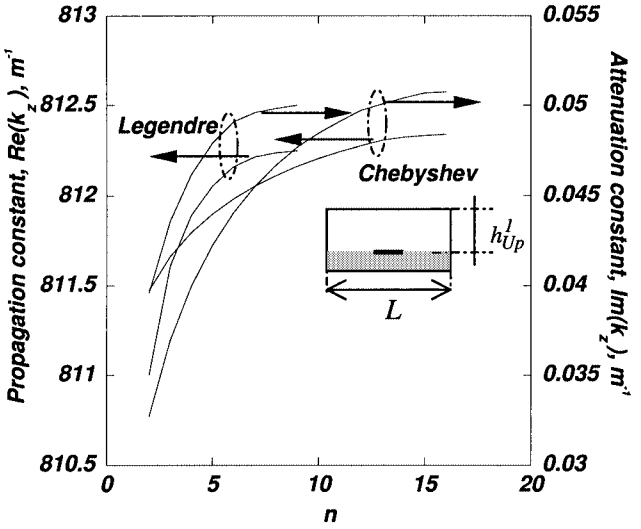


Fig. 4. Propagation constant $\beta$ and attenuation coefficient $\alpha$ versus the number of applied basis functions for a YBCO microstrip line on an $LaAlO_3$ substrate ($f = 10$ GHz). The linewidth $w = 180\ \mu$m, HTS film thickness $t = 0.4\ \mu$m (strip and ground), substrate thickness $h = 0.508$ mm, substrate parameters are $\varepsilon_r = 23.5$, $\tan\delta = 6.0 \cdot 10^{-8}$, the YBCO film characteristics are $\lambda_L = 0.33\ \mu$m, $\sigma_n = 3.0 \cdot 10^6\ \Omega \cdot \mathrm{m}^{-1}$, $L = 8$ mm, $h^1_{\mathrm{Up}} = 5$ mm.

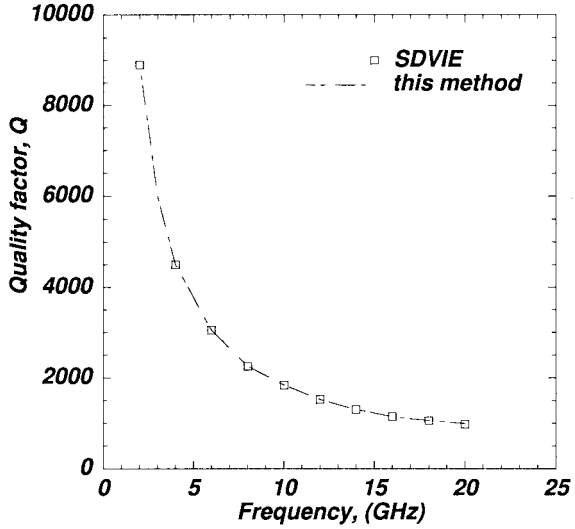


Fig. 5. Calculated $Q$ factor of the YBCO microstrip line on an $LaAlO_3$ substrate versus frequency using this method and SDVIE [6]. The linewidth $w = 20\ \mu$m, HTS film thickness $t = 0.4\ \mu$m, substrate thickness $h = 0.508\ \mu$m, YBCO film characteristics are $\lambda_L = 0.323\ \mu$m, $\sigma_n = 3.5 \cdot 10^6\ \Omega \cdot \mathrm{m}^{-1}$, substrate parameters are the same as in Fig. 4.

where $Y^{i+1}_{h(e)}(h^{i+1})$ is the input load admittance for TE(TM) waves seen from the $i$th layer toward the $(i+1)$th one.

With (28), the expression for the tangential field in the $\boldsymbol{u}, \boldsymbol{v}$ coordinate system at any $j$th interface $(2 \le j \le I(J)+1)$ can be derived as

$$\tilde{E}^j_u = \tilde{E}^1_u \prod_{k=1}^{j-1} K^k_u \text{ and } \tilde{E}^j_v = \tilde{E}^1_v \prod_{k=1}^{j-1} K^k_v. \tag{29}$$

Using back $\boldsymbol{u}, \boldsymbol{v}$ to $\boldsymbol{x}, \boldsymbol{z}$ transformation, one obtains

$$\begin{bmatrix} \tilde{E}^j_z \\ \tilde{E}^j_x \end{bmatrix} = [T]^{-1} \begin{bmatrix} \prod_{k=1}^{j-1} K^k_u & 0 \\ 0 & \prod_{k=1}^{j-1} K^k_v \end{bmatrix} [T] \begin{bmatrix} \tilde{E}^1_z \\ \tilde{E}^1_x \end{bmatrix}. \tag{30}$$

Using (30) together with (26), the power flux spectrum for a structure with an arbitrary number of layers can now be efficiently calculated and used to define the elements of voltage eigenvectors. In order to avoid the calculation of cross powers, the orthogonality condition between voltage and current eigenvectors is used to form a system of linear equations, as in [14]

$$\left.\begin{aligned} P^k &= \frac{1}{2} V^T_k I^*_k \\ 0 &= V^T_l I_m, \qquad l \ne m \end{aligned}\right\}, \qquad k, l, m = 1, \ldots, n. \tag{31}$$

Modal impedances are defined for each $l$th line and each $k$th mode as a ratio between related elements of matrices $[V]$ and $[I]$ in a way that $Z_{l,k} = V_{l,k}/I_{l,k}$ and are used to define the multiport admittance matrix of the coupled-line system [15]. The utility of developed formulas above was demonstrated in the experimentally verified filter design [16].

## III. Numerical Results and Discussion

First, we studied the convergence behavior of Galerkin's method for both sets of basis function. The plot for propagation constants versus the number of applied basis function is shown in Fig. 4 for a superconducting (YBCO) microstrip line. As

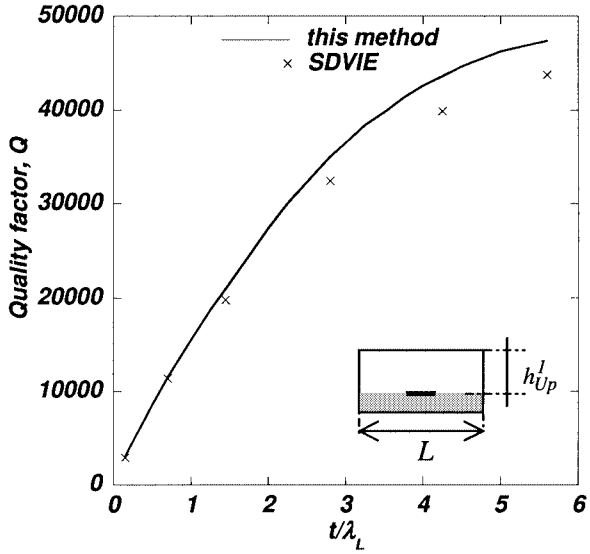


Fig. 6. Calculated quality factor for an Nb microstrip line on an $LaAlO_3$ substrate ($f = 2$ GHz) as a function of the reduced strip thickness using this method and SDVIE [6]. The linewidth $w = 20\ \mu$m, substrate thickness $h = 0.508$ mm, YBCO film characteristics are $\lambda_L = 0.0715\ \mu$m, $\sigma_n = 128 \cdot 10^6\ \Omega \cdot \mathrm{m}^{-1}$.

follows from this figure, the Chebyshev polynomial-based set demonstrates quite poor convergence (typically approximately 15 basis functions have to be applied to get a result with 1% accuracy). This makes this basis set computationally inefficient. The basis set based on the Legendre polynomials shows rather better behavior (7–8 basis functions are enough to obtain a result close to the converged value) and all data presented below are computed using eight basis function of this set. Let us compare the results of simulation of the attenuation coefficient and the propagation constant of the HTS (YBCO) microstrip line on an $LaAlO_3$ substrate obtained by this method with the results of the SDVIE application to the same line [6]. For this purpose, we will use the quality factor of the transmission line $Q = \beta/2\alpha$ as a function of frequency. One indicates an

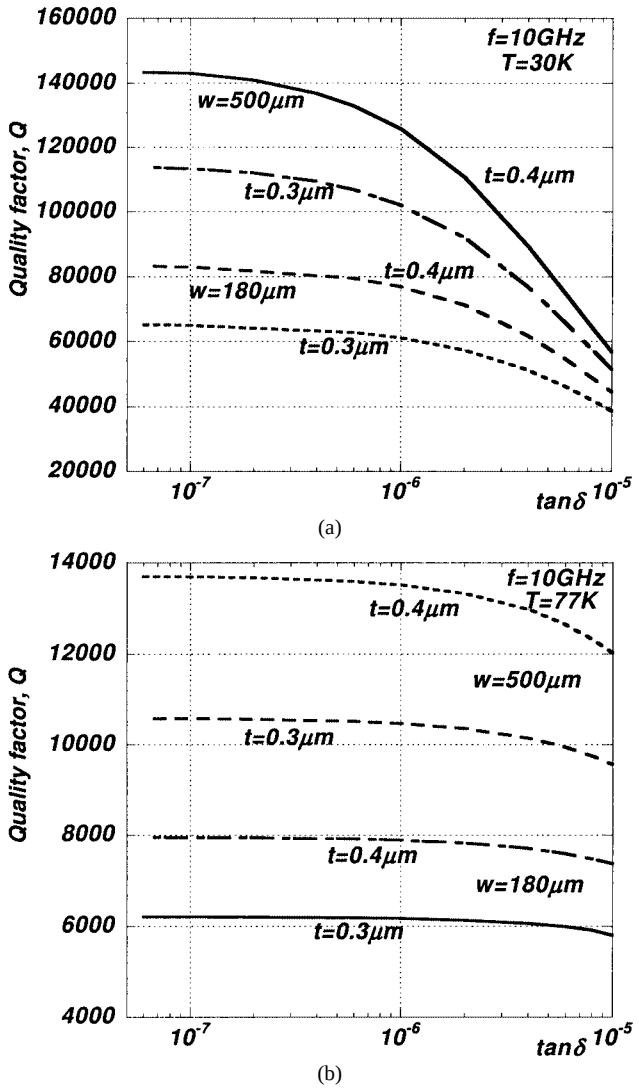


(a)

(b)

Fig. 7. Calculated quality factor of a YBCO microstrip line on an $LaAlO_3$ substrate ($f = 10$ GHz) as a function of $\tan\delta$ of the substrate at: (a) $T = 30$ K [$\lambda_L = 0.170\ \mu$m, $\sigma_n = 3.5 \cdot 10^6\ (\Omega \cdot \text{m})^{-1}$] and (b) $T = 77$ K [$\lambda_L = 0.330\ \mu$m, $\sigma_n = 3.0 \cdot 10^6\ \Omega \cdot \text{m}^{-1}$], the substrate parameters are the same as in Fig. 4.

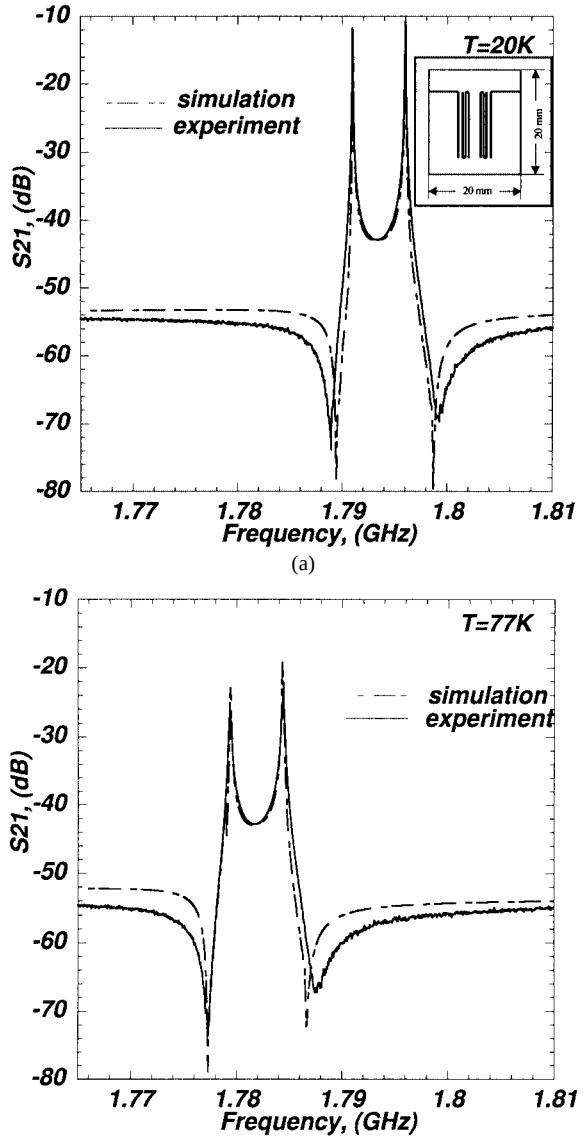


(a)

(b)

Fig. 8. Simulated and measured [17] transmission characteristics of two coupled S-shaped resonators. The dielectric substrate of 0.515-mm thickness was used with parameters $\varepsilon = 23.3$, $\tan\delta = 2.0 \cdot 10^{-6}$, the YBCO film of 0.45-$\mu$m thickness was used with characteristics: (a) $\lambda_L = 0.144\ \mu$m, $\sigma_n = 5.25 \cdot 10^6\ \Omega \cdot \text{m}^{-1}$ and (b) $\lambda_L = 0.282\ \mu$m, $\sigma_n = 12.4 \cdot 10^6\ \Omega \cdot \text{m}^{-1}$.

excellent coincidence between the results of the simulation by these two methods (Fig. 5).

The calculated quality factor $Q$ of an Nb microstrip line on $LaAlO_3$ as a function of film thickness at 2 GHz is plotted in Fig. 6.

The result is shown in comparison with $Q(t/\lambda_L)$ obtained for the same line by the SDVIE method [6]. The results are in good agreement for $t/\lambda_L \leq 2.5$, while for higher values, discrepancy becomes larger approaching a 10% limit at $t/\lambda_L = 5.5$.

The contribution of the dielectric loss into the $Q$ factor of an HTS (YBCO) microstrip line on an $LaAlO_3$ substrate ($\varepsilon_r = 23.5$) is shown in Fig. 7. The calculated results are obtained by the method presented in this paper. The influence of the dielectric loss on the $Q$ factor is well pronounced at a lower temperature [see Fig. 7(a)], when the YBCO film contribution is very small. At a higher temperature [see Fig. 7(b)], the surface resistance of the YBCO film is mainly responsible for the $Q$ factor of the microstrip line and the dependence of the $Q$ factor on $\tan\delta$ of the substrate is smoothed.

The next step was a comparison of results of the calculation of the multistrip structure characteristics by the method developed with the experimental characteristics. The multistrip structure of two coupled S-shaped YBCO resonators on $LaAlO_3$ substrates was simulated and measured. The results of the simulation of the transmission coefficient in comparison with the measured data at two different temperatures ($T = 20$ K and 77 K) [17] are presented in Fig. 8. A good agreement between the simulated and measured data gives a reliable confirmation of correctness of the method developed.

Finally method was used to verify a design of a 12-pole quasi-elliptic filter [see Fig. 9(a)]. The structure of the filter consists of 38 coupled microstrip lines, which are connected in a way to establish 12 S-shaped resonators according to the figure. For the purpose of simulation, a multiport admittance matrix of the array was calculated based on the power–current definition (31).

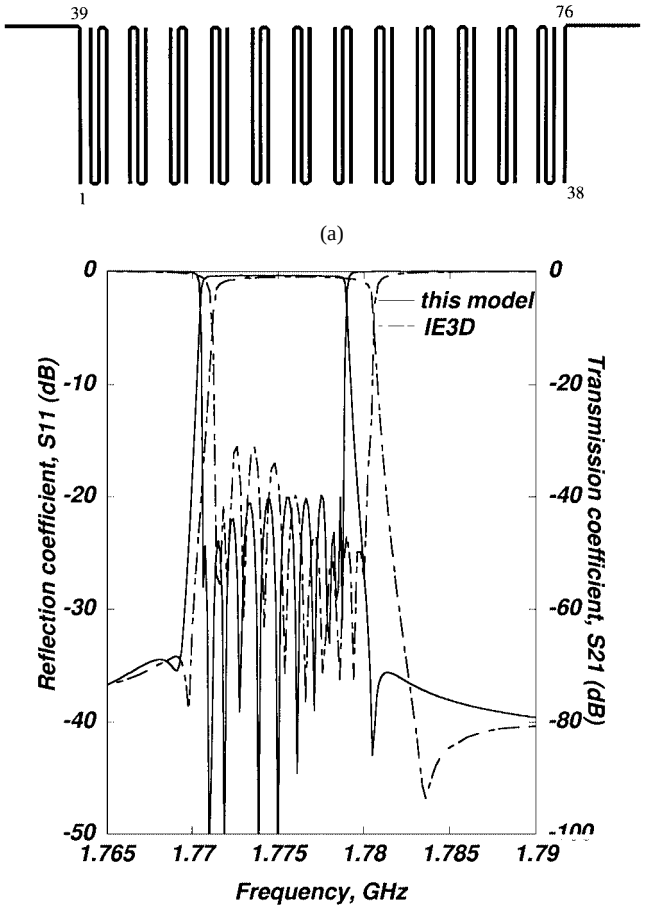


(a)

(b)

Fig. 9. (a) Layout of the 12-pole filter on the S-shaped resonators. (b) Simulated performance of the filter at 60 K using the presented model and IE3D electromagnetic simulator. Parameters of the HTSC used in simulation and box dimensions are the same as in [18].

It has been modified by adding self-admittance and mutual admittance of microstrip interconnectors and open-ended capacitances to the elements, which represent the related nodes of the circuit. The resultant matrix was used to calculate $S$-parameters of the circuit, which are presented in Fig. 9(b), together with the one obtained using an IE3D electromagnetic simulator. One can say that it is difficult to expect better agreement between model-based simulation and a three-dimensional (3-D) electromagnetic one; thus, we consider it as a good argument to confirm confidence to developed codes.

## IV. Conclusions

A computationally efficient full-wave method of analysis of an HTS multistrip multilayered structure has been proposed and discussed. The method allows taking into account real characteristics of the dielectric layers and conducting strips of a finite thickness. Examples of simulation of different structures (Nb microstrip line and YBCO microstrip line on an LaAlO3 substrate, multistrip HTS structure of the narrow-band filter) revealed the high efficiency and reliability of the method. As result, the complex propagation constants and related modal impedances of the multiconductor structure containing superconducting (normal metal) strip and lossy multilayer dielectric can be calculated. The method can be effectively used for a simulation and design of planar filter structures including the tunable devices using a ferroelectric layer.

## Acknowledgment

The authors are greatly indebted to B. Oh, LG Corporate Institute of Technology, Seoul, Korea, Y. H. Choi, LG Corporate Institute of Technology, and B.-C. Min, LG Corporate Institute of Technology, for providing the numerical results of a simulation of the characteristics 12-pole filter obtained by IE3D software. The authors are also very grateful to E. Kollberg, Chalmers University of Technology, Göteborg, Sweden, for his support.

## References

[1] *IEEE Trans. Microwave Theory Tech. (Special Issue)*, vol. 48, pp. 1171–1282, July 2000.

[2] S.-C. Mao, J.-Y. Ke, and C. H. Chen, "Propagation characteristics of superconducting microstrip lines," *IEEE Trans. Microwave Theory Tech.*, vol. 44, pp. 33–41, Jan. 1996.

[3] J. M. Pond, C. M. Krowne, and W. L. Carter, "On the application of complex resistive boundary conditions to model transmission lines consisting of very thin superconductor," *IEEE Trans. Microwave Theory Tech.*, vol. 37, pp. 181–190, Jan. 1989.

[4] D. Nghiem, J. T. Williams, and D. R. Jackson, "A general analysis of propagation along multiple-layer superconducting stripline and microstrip transmission lines," *IEEE Trans. Microwave Theory Tech.*, vol. 39, pp. 1553–1565, Sept. 1991.

[5] L. H. Lee, S. M. Ali, and W. G. Lyons, "Full-wave characterization of high-$Tc$ superconducting transmission lines," *IEEE Trans. Appl. Superconduct.*, vol. 2, pp. 49–57, June 1992.

[6] L. H. Lee, S. M. Ali, W. G. Lyons, D. E. Oates, and J. D. Goettee, "Analysis of superconducting transmission line structures for passive microwave device applications," *IEEE Trans. Appl. Superconduct.*, vol. 3, pp. 2782–2787, Mar. 1993.

[7] L. H. Lee, W. G. Lyons, T. Orlando, S. M. Ali, and R. S. Withers, "Full-wave analysis of superconducting microstrip lines on anisotropic substrates using equivalent surface impedance approach," *IEEE Trans. Microwave Theory Tech.*, vol. 41, pp. 2359–2367, Dec. 1993.

[8] S. Amari, "Comments on 'On the application of complex resistive boundary conditions to model transmission lines consisting of very thin superconductor'," *IEEE Trans. Microwave Theory Tech.*, vol. 43, p. 912, Apr. 1995.

[9] I. B. Vendik, O. G. Vendik, A. N. Deleniv, V. V. Kondratiev, M. N. Goubina, and D. V. Kholodniak, "Development of CAD tool for a design of microwave planar HTS filters," *IEEE Trans. Microwave Theory Tech.*, vol. 48, pp. 1247–1255, July 2000.

[10] C. S. Gorter and H. B. G. Casimir, *Phys. Z*, vol. 35, p. 963, 1934.

[11] T. Itoh, "Spectral domain immitance approach for dispersion characteristics of generalized printed transmission lines," *IEEE Trans. Microwave Theory Tech.*, vol. MTT-28, pp. 733–736, July 1980.

[12] N. K. Das and D. M. Pozar, "Full-wave spectral-domain computation of material, radiation, and guided wave losses in infinite multilayered printed transmission lines," *IEEE Trans. Microwave Theory Tech.*, vol. 39, pp. 54–63, Jan. 1991.

[13] G. Cano, F. Medina, and M. Horno, "On the efficient implementation of SDA for boxed strip-like and slot-like structures," *IEEE Trans. Microwave Theory Tech.*, vol. 46, pp. 1801–1806, Nov. 1998.

[14] ——, "Efficient spectral domain analysis of generalized multistrip lines in stratified media including thin, anisotropic, and lossy substrates," *IEEE Trans. Microwave Theory Tech.*, vol. 40, pp. 217–227, Feb. 1992.

[15] V. K. Tripathi and H. Lee, "Spectral domain computation of characteristic impedances and multiport parameters of multiple coupled microstrip lines," *IEEE Trans. Microwave Theory Tech.*, vol. 37, pp. 215–221, Jan. 1989.

[16] A. Deleniv, M. Gashinova, I. Vendik, and A. Eriksson, "Designing of an interdigital hairpin band-pass filter utilizing a model of coupled slots," *IEEE Trans. Microwave Theory Tech.*, vol. 50, pp. 2153–2158, Sept. 2002.

[17] A. Deleniv, D. Kholodniak, A. Lapshin, I. Vendik, P. Yudin, B.-C. Choi, and B. Oh, "Extracting the model parameters of high-temeperature superconductor film microwave surface impedance from the experimental characteristics of resonators and filters," *Superconduct. Sci. Technol.*, vol. 13, pp. 1419–1423, Oct. 2000.

[18] I. Vendik, A. Deleniv, V. O. Sherman, A. A. Svishchev, V. V. Kondratiev, D. V. Kholodniak, A. V. Lapshin, P. Yudin, B.-C. Min, Y. H. Choi, and B. Oh, "Narrow-band Y–Ba–Cu–O filter with quasi-elliptic characteristic," *IEEE Trans. Applied Superconduct.*, vol. 11, pp. 477–480, Mar. 2001.

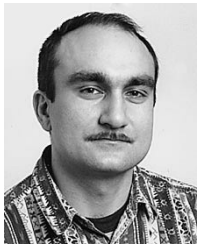

**Anatoli N. Deleniv** was born in the Ukraine, in 1969. He received the Radio Engineering Diploma degree (with honors) and Ph.D. degree from St. Petersburg Electrotechnical University, St. Petersburg, Russia, in 1996 and 1999 respectively.

Since 2000, he has been with the Department of Microelectronics, Chalmers University of Technology, Göteborg, Sweden, where he is currently a Post-Doctoral Researcher. His research interest is mainly in development of models for planar microwave structures suitable for CAD of microwave integrated circuits and design of passive microwave components based on HTSs and ferroelectric materials.

**Marina S. Gashinova** received the Diploma degree (with honor) in mathematics and mechanics and B.S. degree in physics from St. Petersburg Electrotechnical University, St. Petersburg, Russia, in 1991 and 1997, respectively, and is currently working toward the Ph.D. degree at St. Petersburg State University.

Since December 1999, she has been with the Department of Microelectronics and Radio Engineering, St. Petersburg Electrotechnical University. Her main fields of interest include boundary value problems in electromagnetic theory, wave propagation through anisotropic media, and filter design. She is currently engaged in the analysis of planar transmission lines embedded in anisotropic materials and multiconductor transmission lines.

**Irina B. Vendik** (M'96) received the Electronics Engineer Diploma and Candidate of Sc. (Ph.D.) degree from the Leningrad Electrical Engineering Institute (now St. Petersburg Electrotechnical University), St. Petersburg, Russia, in 1959 and 1964, respectively, and the D.Sc. (Phys.) degree from the A. F. Ioffe Physicotechnical Institute, St. Petersburg, Russia, in 1990.

She is currently a Professor with the Department of Microelectronics and Radio Engineering and Head of the Microwave Computer-Aided Design Group, St. Petersburg Electrotechnical University. Her general research interest have been in foundations of solid-state physics and microwave electronics including low-dimensional crystals at microwave, p-i-n diode switches and phase shifters, and microwave applications of HTSs. Her current activity is in the area of elaboration of HTS microwave components including resonators, filters, power dividers, switches, and phase shifters. She is also interested in the development of CAD-oriented models of HTS planar components in linear and nonlinear approaches.